

UC Merced

UC Merced Previously Published Works

Title

Registry Kinetics of Myosin Motor Stacks Driven by Mechanical Force-Induced Actin Turnover

Permalink

<https://escholarship.org/uc/item/92s605bn>

Journal

Biophysical Journal, 117(5)

ISSN

0006-3495

Authors

Dasbiswas, Kinjal
Hu, Shiqiong
Bershadsky, Alexander D
et al.

Publication Date

2019-09-01

DOI

10.1016/j.bpj.2019.07.040

Peer reviewed

Registry Kinetics of Myosin Motor Stacks Driven by Mechanical Force-Induced Actin Turnover

Kinjal Dasbiswas,^{1,*} Shiqiong Hu,^{2,3} Alexander D. Bershadsky,^{3,4} and Samuel A. Safran⁵

¹Department of Physics, University of California, Merced, California; ²Department of Pharmacology, University of North Carolina at Chapel Hill, Chapel Hill, North Carolina; ³Mechanobiology Institute, National University of Singapore, Singapore, Singapore; ⁴Department of Molecular Cell Biology and ⁵Department of Chemical and Biological Physics, Weizmann Institute of Science, Rehovot, Israel

ABSTRACT Actin filaments associated with myosin motors constitute the cytoskeletal force-generating machinery for many types of adherent cells. These actomyosin units are structurally ordered in muscle cells and, in particular, may be spatially registered across neighboring actin bundles. Such registry or stacking of myosin filaments have been recently observed in ordered actin bundles of even fibroblasts with super-resolution microscopy techniques. We introduce here a model for the dynamics of stacking arising from long-range mechanical interactions between actomyosin units through mutual contractile deformations of the intervening cytoskeletal network. The dynamics of registry involve two key processes: 1) polymerization and depolymerization of actin filaments and 2) remodeling of cross-linker-rich actin adhesion zones, both of which are, in principle, mechanosensitive. By calculating the elastic forces that drive registry and their effect on actin polymerization rates, we estimate a characteristic timescale of tens of minutes for registry to be established, in agreement with experimentally observed timescales for individual kinetic processes involved in myosin stack formation, which we track and quantify. This model elucidates the role of actin turnover dynamics in myosin stacking and explains the loss of stacks seen when actin assembly or disassembly and cross-linking is experimentally disrupted in fibroblasts.

SIGNIFICANCE Organization of the cellular cytoskeleton into ordered structures is important for various biological processes involving mechanical forces, such as muscle contraction and cell division. Here, we theoretically show how mechanical forces communicated through the intervening cytoskeletal network can drive myosin motors into stacks across neighboring stress fibers. We quantitatively analyze some key processes involved in myosin stacking observed in recent microscopy experiments. These analyses support our theoretical model for the force-induced reorganization of actin in stress fibers, which we predict should take tens of minutes. The proposed kinetic mechanism involves the force-dependent remodeling of actin polymers and adhesion regions.

INTRODUCTION

Cells employ forces generated through the physicochemical activity of the molecular motor myosin associated with the actin cytoskeleton to accomplish a variety of tasks, notably, muscle contraction and cell motility (1). The structural order of the cellular cytoskeleton is sensitive to mechanical cues (2), as demonstrated experimentally in cells cultured on soft deformable substrates (3,4). Theory that describes cellular contractility in terms of force dipoles embedded in an elastic medium (5,6) links such order, for example,

striation in muscle cells (7), to mechanical interactions mediated by an elastic substrate (8,9).

The most pronounced cytoskeletal structures associated with myosin II motors are the organized, elastic, parallel actin bundles characteristic of polarized fibroblast cells known as stress fibers (10). Recently, sarcomere-like extensive structural order, including long-range stacking of bipolar myosin II filaments across neighboring stress fibers (11) (resembling the registry of muscle fibrils in striated muscle), was observed in nonmuscle cells using super-resolution microscopy (11–14). The main observations about the self-organization of myosin II filaments in (11) can be summarized as follows (see Fig. 1):

- The stress fibers show “quasisarcomeric” order, in which nonmuscle myosin filaments are distributed in a nearly periodic fashion along the fiber, are oriented parallel to

Submitted February 26, 2019, and accepted for publication July 23, 2019.

*Correspondence: kdasbiswas@ucmerced.edu

Editor: Michael Ostap.

<https://doi.org/10.1016/j.bpj.2019.07.040>

© 2019 Biophysical Society.

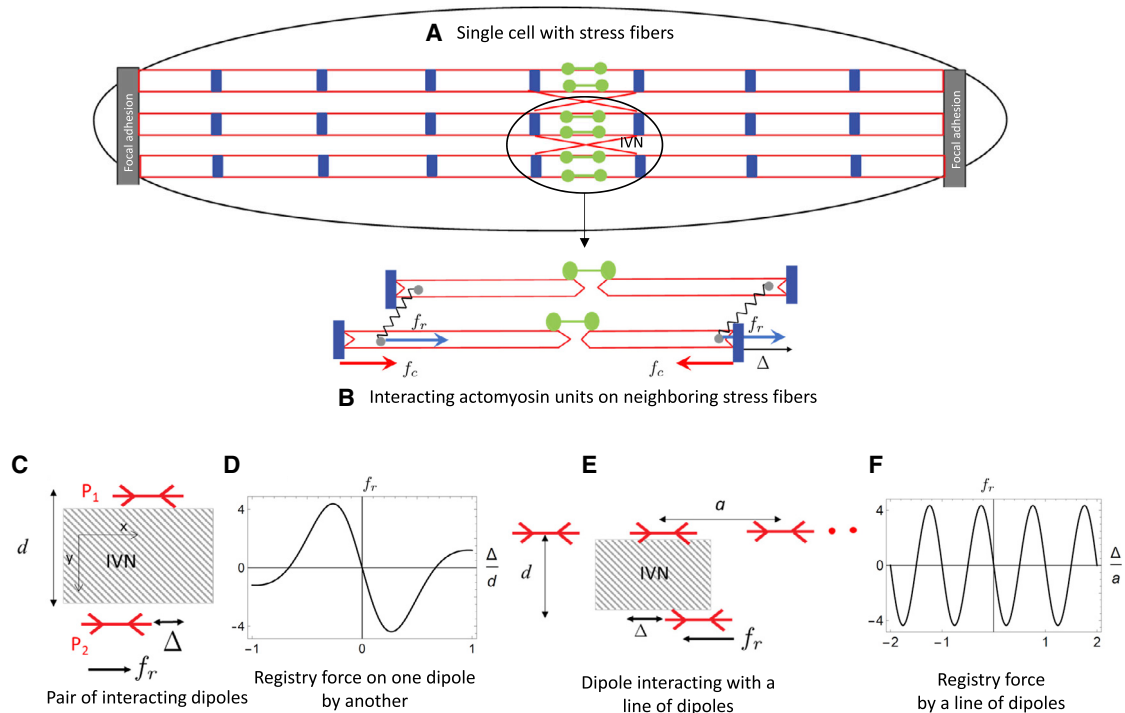


FIGURE 1 Stress fiber registry and theory of elastic interactions. (A) A schematic of a few stress fibers in an entire cell is given. Each stress fiber is anchored at their ends to the substrate through focal adhesions (gray bars) and comprises a series of actomyosin units with a sarcomere-like configuration. Within each unit, actin filaments (red) are associated with bipolar myosin filaments (green) alternating with α -actinin cross-linkers (blue). (B) A schematic of two actomyosin units (“sarcomeres”) on neighboring stress fibers is given. Each unit comprises pairs of antiparallel actin filaments (only one representative pair of actin filaments is shown for clarity) connected at their barbed ends to adhesion regions comprising cross-linkers (blue), whereas their pointed ends are associated with myosin filaments (green). Two such actomyosin units on neighboring stress fibers are mechanically connected through a cytoskeletal intervening network (IVN), represented here as springs. The pairwise contractile forces generated by myosin acting on actin, f_c , are exerted on the elastic IVN (stretched springs), which then transmits these forces to other fibers. (C) A schematic representation of the situation in (B) is given in which the two actomyosin units, misregistered by a distance, Δ , along the stress fibers, and separated by a transverse distance, d , are each modeled as a force dipole—a pair of equal and opposite forces (5)—exerted on the IVN. (D) Dependence of registry force on lower dipole (P_2) in (C) on the distance by which actomyosin units are misregistered, Δ , relative to the separation, d , is shown. (E) Interaction of a single actomyosin unit with a neighboring stress fiber is shown, modeled as a periodic array of dipoles (of period spacing, a , corresponding to the sarcomere size). (F) Dependence of registry force on single, lower dipole in (E) on the distance by which it is misregistered from the dipoles in the line, Δ , relative to the separation, a , of the dipoles in the line is shown. To see this figure in color, go online.

the actin filaments, and colocalize with the pointed (minus) ends of the actin. Along the actin, myosin alternates with regions enriched in the actin cross-linker protein, α -actinin, which is localized at the barbed (plus) end of actin.

- The myosin filaments show a second level of long-range organization, wherein they stack across parallel and distinct stress fibers that are separated by ~ 100 nm. This resembles the registry of sarcomeres across muscle fibers.
- Such stacking crucially depends on myosin contractile activity, actin polymerization dynamics, and long-range movements of actomyosin.
- The kinetic processes of cytoskeletal reorganization that lead to the formation of myosin stacks take tens of minutes.

Though stress-fiber-associated molecules such as myosin 18B have been found necessary for stacking (15), and other local effects such as “splitting” of myosin filaments could be involved (12), stacking across several actin bundles not

in direct contact suggests a long-range driving force behind the formation and maintenance of such stacks in the noisy cellular environment characterized by stochastic forces. Mechanical forces have been found to be crucial for the registry of myofibrils in striated muscle in both tissue culture (16) and in vivo in insect flight muscle (17). That myosin stack formation requires both actomyosin contractile activity and actin filament turnover (11) leads us to a unifying proposal for structural order driven by mechanical forces arising in both muscle and nonmuscle cells (18). These forces may be transmitted by a mechanical medium that could be a soft external substrate in cell culture experiments (4) or the disordered cytoskeletal network itself, which intervenes between and mechanically couples neighboring actin bundles (11).

The theory for registry driven by mechanical interactions predicts that the registered configuration of actomyosin elements is the mechanical equilibrium state of the material medium connecting neighboring actin bundles (8,18). In

this work, we introduce the kinetics of registry and compare it with experimental data obtained by tracking the myosin movements as they stack. For these actomyosin elements to move into registry, some of the actin polymers in a bundle associated with the myosin filament must depolymerize while the others must polymerize; without that, the myosin filaments are sterically hindered from moving, and registry cannot arise. Actin, like many other biological macromolecules, is mechanosensitive, in that its structural conformations are modulated by the mechanical forces acting on it (19). This is particularly the case for cytoskeletal actin *in vivo*, where actin is associated with many other actin-binding proteins. Here, we propose a minimal model by which ATP-dependent, myosin-generated contractile forces in one actin bundle can be communicated to a distant actin bundle through the intervening cytoskeletal medium to which both these bundles are attached through “adhesion zones” comprising cross-linkers (a key component of sarcomeric organization). This mechanical force may then modulate the rates of polymerization and depolymerization of the actin polymers in that distant bundle. The asymmetry in the dependence of polymerization kinetics on tensile and compressive forces leads to the effective translocation of the actin bundles toward an eventually registered configuration. The model elucidates the processes involved in the self-organization of actin and myosin during the development of both stress fibers in fibroblasts (11) and myofibrils in muscle cells (20). How the cytoskeletal machinery assembles into functional structures is a question of general interest, and here, we uncover some specific processes involved in such self-organization through modeling and quantitative analysis of microscopy experiments.

MATERIALS AND METHODS

Experimental methods

Cell culture and transfection

Rat embryonic fibroblasts (REF52 cells) established by the group of W. Topp at Cold Spring Harbor Laboratory (21) were cultured in Dulbecco's modified Eagle's medium (11965092; Thermo Fisher Scientific, Waltham, MA) containing 10% fetal bovine serum (FBS; 10082147; Thermo Fisher Scientific) at 37°C in 5% CO₂ incubator as described previously (11). Electroporation (Neon; Thermo Fisher Scientific) was applied for transient transfection following manufacturer's protocol. The plasmids used were F-Tractin-tdTomato, myosin regulatory light chain (RLC)-GFP, and α -actinin-1-mCherry, as described previously (11). Overnight after transfection, the cells were replated on 10 μ g/mL fibronectin-coated high-precision glass coverslips (No. 1.5H, 017650 Marienfeld coverslips (Lauda-Königshofen, Germany) cleaned as described previously (11)) and incubated for 24 h before imaging.

Imaging using Nikon structured illumination microscopy

The coverslip was transferred to an observation chamber (CM-B25-1 Chamliide magnetic chamber; Live Cell Instruments, Seoul, South Korea) and changed to fresh imaging medium (Leibovitz's medium with 10% fetal

bovine serum and 1% penicillin-streptomycin). The Nikon structured illumination microscopy (N-SIM) images were captured with dual color (laser 488 and laser 561) SIM mode using a 100 \times oil (NA 1.49) objective, with autofocus maintained by the Nikon Perfect Focus system. The samples were mounted in a humidified cell culture chamber and maintained at 37°C with 5% CO₂. The interval times of images were 30 s or 1 min for live-cell imaging.

The quantitative analysis of these images was performed by manually tracking positions of myosin filaments with the ImageJ software (using the “point-and-click” method).

Theoretical methods

In (11), it was shown experimentally that bipolar myosin II filaments bound to pointed ends of antiparallel actin filaments in neighboring actin bundles tend to register into “stacks” that can extend across as many as five separate actin bundles, typically organized into stress fibers as shown in Fig. 1. This is a dynamic process: myosin filaments that were initially not registered with those on neighboring (but distant and distinct) fibers tended to move into mutual registry on the scale of tens of minutes (11). A mechanism for registry that is independent of (as yet unobserved) direct molecular bridges between the myosin in different stress fibers is related to the mechanical deformation of the disordered, intervening network (IVN) of cytoskeletal components by the contractile actomyosin units in the two adjacent fibers, typically separated by a few hundred nm, as shown in Fig. 1. Indeed, a region of loosely organized actin connecting two neighboring stress fibers is revealed under super-resolution microscopy (11,22). These mechanical deformations of the IVN are long-ranged and can lead to stacking of myosins over distances of the order of a micrometer. The IVN can transmit mechanical forces from a stress fiber under tension because of myosin contractility to another.

Actomyosin mechanical interactions modeled as elastic force dipoles

Myosin filaments bound to actin filaments generate active contractile forces via ATP-hydrolysis (1) that induce tension in the actin filaments joined by cross-linkers. Such actomyosin units can be minimally modeled as force dipoles (5), i.e., pairs of equal and opposite forces, that are coupled to (via the cross-linkers) and deform the IVN and cellular cytoskeleton. The pair of contractile forces act at the points at which each actomyosin unit connects with the surrounding mechanical medium, here the cytoskeletal IVN. Two such force dipoles on neighboring stress fibers, such as \mathbf{P}_1 and \mathbf{P}_2 shown in Fig. 1, may interact through their mutual deformations of the mechanical medium (here, the IVN), in which they induce a displacement \mathbf{u} . The net elastic energy of deformation of the IVN corresponds to the work done by one dipole, say \mathbf{P}_2 , against the deformation induced by the other, \mathbf{P}_1 . This is thus an indirect interaction of the actomyosin units that is induced by the intervening elastic medium, which in turn is deformed by these actively contractile units. This interaction has similar features for force dipoles in both two and three dimensions (see Supporting Materials and Methods). Because the dipoles are oriented in the x -direction (along the stress fiber) in this geometry, the elastic energy of the IVN depends only on the deformation in this direction. The medium then exerts a force on dipole \mathbf{P}_2 because of the deformation created in it by dipole \mathbf{P}_1 so as to minimize its overall deformation. The component of this force along the stress fiber, originating in the long-range elastic interaction between two force dipoles mediated by the medium, is given by (5,8,9)

$$f_r(\mathbf{x}) = -P_2 \frac{\partial^2 u_x}{\partial x^2} = \frac{1+\nu}{\pi E} P_1 P_2 \frac{\partial^3}{\partial x^3} \left((1-\nu) \frac{1}{|\mathbf{x}|} + \nu \frac{x^2}{|\mathbf{x}|^3} \right), \quad (1)$$

where \mathbf{x} is the displacement of \mathbf{P}_2 relative to \mathbf{P}_1 (see Fig. 1) and the deformation is calculated using linear elastic theory for an isotropic medium (23). In the geometry considered in Fig. 1, $\mathbf{x} = (\Delta, d)$, where Δ is the misregistry that separates the dipoles in the direction parallel to their respective stress fibers and d is the transverse distance between the two dipoles corresponding to the spacing between neighboring stress fibers. The relevant elastic constants are the Young's modulus, E , and Poisson's ratio, ν , of the cell's cytoskeleton (specifically, the IVN), which, over the timescales of interest (less than a second for force transmission (24)), can be considered nearly incompressible ($\nu \approx 0.5$). The force in Eq. 1 tends to move the neighboring dipoles into registry, where $\Delta = 0$ as shown in Fig. 1 C. If $\Delta > 0$, that is, \mathbf{P}_2 is shifted away from \mathbf{P}_1 in one direction, then the force from the medium on \mathbf{P}_2 , because of the deformations induced by \mathbf{P}_1 , acts in the opposite (negative x -) direction, tending to push it toward registry at $\Delta = 0$. Intuitively, because actomyosin activity-induced force dipoles are contractile, the cytoskeletal (including IVN) elastic forces will tend to localize them to regions of the IVN that are more stretched at mechanical equilibrium. Similarly, an IVN-induced force component can also develop in the y -direction: $f_y(\mathbf{x}) = -P_2(\partial^2 u_x / \partial x \partial y)$, which can be attractive over a range of separations. This is detailed in the Supporting Materials and Methods. The magnitude of the IVN-induced mechanical force between a pair of dipoles restricted to be on neighboring stress fibers then scales as $f \sim P^2 / (\pi E d^4)$.

Although the stacking of short, individual actomyosin filaments is driven by the interactions of a pair of force dipoles, this same picture may also be extended to describe the interactions between collections of dipoles that model the entire stress fiber. For a periodic array of dipoles (each of magnitude P) representing a stress fiber with nearly periodic occurrence of myosin filaments ("quasimeric" order), the registry force on a single neighboring actomyosin unit is given by (8,9)

$$f_r(\Delta) = P^2 / (E a^4) \times \phi(d/a, \nu) \times \sin(2\pi\Delta/a), \quad (2)$$

where, as shown in Fig. 1 E, a is the size of each actomyosin unit (or equivalently, the spacing between myosin filaments along the stress fiber), d is the transverse distance between neighboring stress fibers, and ϕ is a transverse coupling factor that depends on the separation, d , of the stress fibers and the Poisson's ratio of the elastic medium (8). These expressions are derived in detail in the Supporting Materials and Methods.

Force-induced actin polymerization and depolymerization

Actin filaments undergo continuous net polymerization and depolymerization at their barbed (plus) and pointed (minus) ends (25) as shown in Fig. 2. They are in dynamic steady state with actin monomers in the ambient solution. In the cellular cytoskeleton in vivo, a variety of actin-binding proteins such as cross-linkers help to maintain stable actin bundles such as stress fibers, at a constant average length. Such an average steady state of actin filaments requires stable adhesions and a balance of the rates of polymerization and depolymerization. For an actin bundle to change length and effectively translocate as required for registry dynamics, these steady-state rates must necessarily be modified.

The various rates of actin polymerization and depolymerization of a single actin polymer (26) are shown in Fig. 2. The rates are different at the barbed (plus) and pointed (minus) ends of the actin polymer and also depend on whether the actin monomer being added or removed is bound to ATP or ADP. The rate for polymerization at an ATP-associated barbed (plus) end is much higher than that at an ADP-dependent pointed (minus) end, $k_{on}^+ / k_{on}^- \sim 70$, whereas the corresponding ratio of off rates is much smaller ($k_{off}^+ / k_{off}^- \sim 5$). We focus on the predominant situation of ATP-dependent rates at the barbed (plus) end and ADP-dependent rates at the pointed (minus) end. These are the fastest rates that contribute dominantly to the actin filament turnover and set an upper bound on the rate of registry kinetics.

Although actin polymerization is known to generate protrusive forces that drive cell locomotion (27), local thermodynamics predict that an

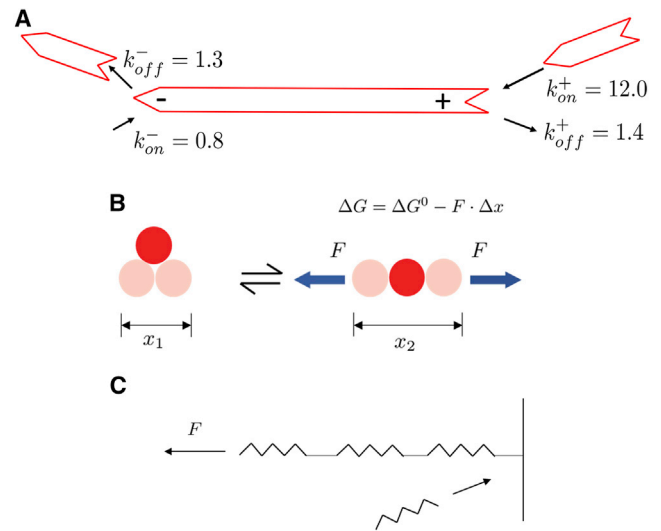


FIGURE 2 Actin polymerization and depolymerization rates and their force dependence. (A) A cartoon representing the various on and off rates of G-actin monomers at either end of an actin polymer is given. The pointed or "minus" end is on the left and undergoes net depolymerization. The rate also depends on whether the actin monomer is bound to ADP or ATP. Here, we show the rates corresponding to ATP-associated monomers at the barbed (plus) end and ADP-associated rates at the pointed (minus) end of an actin polymer. On rates are given in $\mu\text{M}^{-1} \text{s}^{-1}$ and off rates in s^{-1} (25,26). (B) Force dependence of actin polymerization is shown: if an actin polymer anchored at its barbed end is stretched by a tensile force, the force aids the polymerization process by reducing the free-energy barrier for the molecular conformation change occurring during the incorporation of a G-actin monomer (red disk) at the barbed end (28). (C) The mechanical model illustrating the force-dependent polymerization suggested in (B) is given. Each actin bundle (containing actin filaments and cross-linkers) can be represented in a "coarse-grained" sense as a series of beads connected by springs. Under tension (compression), the springs are stretched (compressed), and this strain per spring can be reduced by adding (removing) a spring, which then shares the tensile (compressive) load, F . To see this figure in color, go online.

external force can modify the rates of polymerization (28–30). In particular, a tensile (compressive) force acting on an actin polymer anchored at an end is expected to enhance the rate of polymerization (depolymerization) at that end, by a factor proportional to $\exp(fb/kT)$. Here, f is the force acting on the actin filament, b is related to the monomer size (whose actual projected length is half the monomer size because an actin polymer is a two-stranded helix (1)), and kT is the thermal energy scale. This Arrhenius factor corresponds to the change in the free-energy barrier to monomer addition or removal by work done by a mechanical force and was also suggested in the context of force-dependent unbinding of cell adhesion molecules (31). This mechanical work is the product of the applied force and a displacement corresponding to the addition (removal) of an actin monomer (which is related to monomer size). This change in rates therefore also depends on the sign of the applied force. A tensile force tends to stretch (extend) the actin chain—including cross-linkers—which, for a fixed number of actin monomers, results in individual monomers moving further apart than their equilibrium density. This can be compensated by adding more monomers to the chain, as depicted schematically in Fig. 2 C. A compressive force correspondingly favors depolymerization. Experimentally, mechanical-force-dependent effects on actin assembly have been observed in the formin-mediated polymerization of single actin filaments (32–34) and in branched actin networks (35). These situations resemble actin polymerization phenomena in cells, for example, during cell spreading, when growing actin filaments push the cell membrane forward (36). Similar ideas

have been proposed to drive the force-driven reorganization of focal adhesions that anchor stress fibers in cells to the substrate (37). Although these experimental situations rely on specific molecular actors, we rely here on a general thermodynamic argument independent of a specific molecular mechanism.

Myosin registry kinetics

Because the myosin filament is bound (on average) to the pointed (minus) ends of pairs of antiparallel actin polymers (see Fig. 3), it can only move into registry if the actin polymers effectively translocate, carrying the myosin along with it. The actin polymers are bound on their plus ends to the cross-linkers (blue lines in Fig. 3), which are analogous to Z bodies in muscle sarcomeres (1). The cross-linkers form “adhesion regions” where different actin polymers are bound together. Each actin bundle is made up of 10–100 actin polymers, which prevents their buckling under small compressive forces (38). For illustrative purposes, we represent the entire bundle of cross-linked polymers by these two chains as shown in Fig. 3. There are thus several steps involved in the kinetics of myosin registry:

- 1) Mechanical forces are exerted by the myosin associated with a neighboring actin bundle (labeled A in Fig. 3) on a misregistered actomyosin unit (labeled B in Fig. 3) through the IVN. For simplicity of presentation, we consider A to be fixed, whereas B can move into registry (myosin stacking) with A. The IVN connects with actin polymers at points marked as gray circles near the α -actinin-rich adhesion region (blue). In practice, this point of attachment of the IVN as well as the α -actinin-rich zones have finite width, but we idealize them in these

- cartoons to lie at a specific point because the cross-linkers are known to localize to the plus end of the actin polymer. The deformation of the IVN by myosin-generated contractile forces is represented here by stretched springs. In mechanical equilibrium, these springs align along the vertical direction and are unstretched. This registry force mediated by the IVN acts on the actin polymers in the actomyosin unit B, stretching the left polymers and compressing the right ones at their plus ends.
- 2) The forces on the actin polymers within the unit in B lead to enhanced polymerization of the left and enhanced depolymerization of the right actin polymers. This change in rates of monomer addition or removal depends on the work done by the mechanical forces (28). The myosin filament in B is thus effectively moved to the right toward registry with the myosin filament in A. This also results in partial relaxation (closer to vertical) of the “registry springs” through a shift in the points of attachment of the IVN to the actin polymer.
- 3) The registry forces acting through the IVN are then communicated through the adhesions (blue) to the “rest of” the stress fiber (dashed red lines), which is first stretched to the left and compressed to the right. At long timescales, the stress fibers can remodel and change length to relax this stored stress. The stacking of the myosin filaments is then completed by the motion of the rest of the stress fiber reflected in the translocation of the adhesions, which requires remodeling of the adhesion regions through unbinding and binding of the α -actinin cross-linkers. Thus, both the unequal polymerization of actin polymers within the actomyosin unit and the effective motion of the adhesion, together with the rest of the stress fiber, can move the myosin filament in B to stack (register) with the myosin filament in A. The “registry springs”

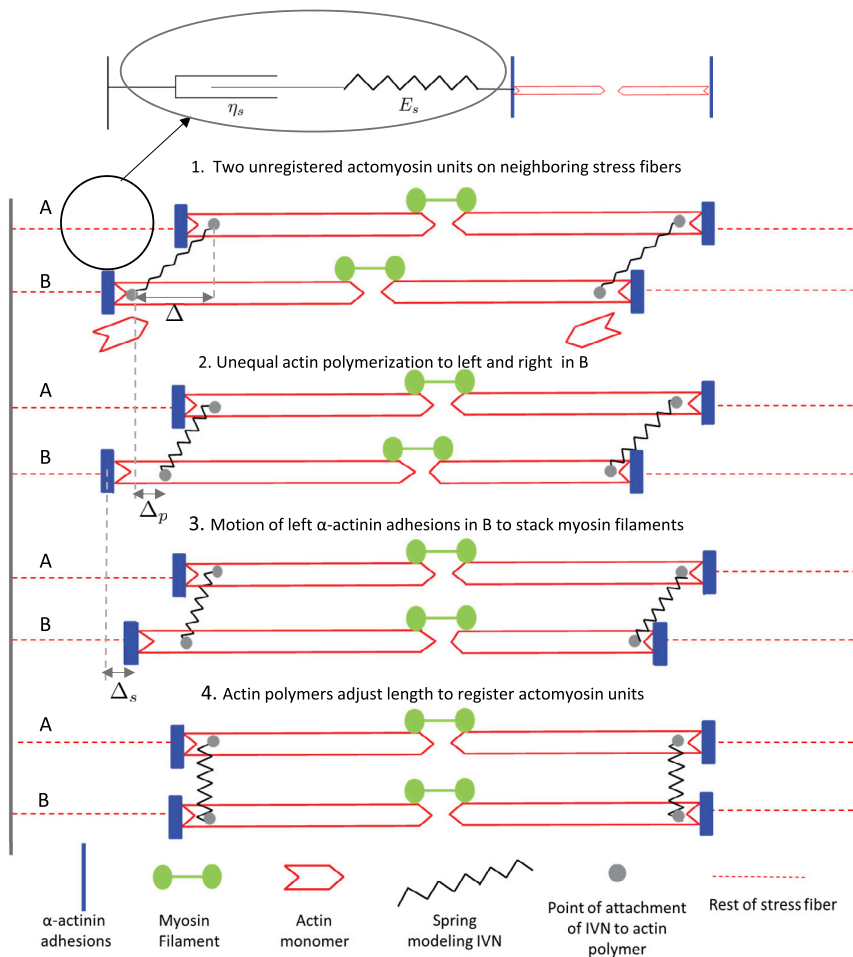


FIGURE 3 For a Figure360 author presentation of Fig. 3, see the figure legend at <https://doi.org/10.1016/j.bpj.2019.07.040>. Figure360

Myosin registry across stress fibers. A cartoon showing myosin filaments (green) associated with neighboring actin bundles (red) held together with α -actinin cross-linker-rich “adhesion zones” (blue) is given. We have shown only one representative actin polymer and myosin filament on each side, but each bundle comprises several actin polymers and associated myosin filaments. The neighboring actin bundles A and B are not in direct contact and are physically connected only through a disordered, cytoskeletal IVN between them. This connection, through the IVN leads to mechanical forces between the actin polymers represented by stretched springs (gray), connecting actin polymers in A and B at points of attachment shown as gray circles. This registry force from one actomyosin unit (labeled A) acts on another actomyosin unit (labeled B) on a neighboring stress fiber and leads to the dynamics of B shown here, which may be broken down into several different steps (not necessarily occurring in this sequence). The inset shows the viscoelastic model for the dynamics of the rest of the stress fiber attached to B (a spring and a dashpot in series, with elasticity and viscosity indicated). To see this figure in color, go online.

are completely relaxed when this state of mechanical equilibrium is reached.

- 4) Although the registry of the two actomyosin units A and B is already complete, the final state may be one where the length of the actin polymers to the left and the right have equalized. These steady-state lengths of the actin polymers are maintained within the cell by a variety of actin-associated proteins not described by our model. The property of the stress fibers that they flow and remodel at long timescales is crucial for the registry of the adhesion sites and the final equalization of the length of the actin polymers.

We note that this stepwise description and the picture of an actomyosin unit A moving with respect to a fixed actomyosin unit B serve a conceptual purpose by identifying the various factors at play and are not necessarily the sequence in which these processes occur. The lengthening or shortening of actin polymers within a “sarcomere,” for example, are likely to happen simultaneously with the remodeling of the rest of the stress fiber, though the timescales involved are in principle different.

We now estimate the changes in polymerization rates caused by the registry forces mediated by the deformation of the IVN (8,9). The rate-limiting step depends on the longest timescale, which, in our case, is the depolymerization from the ADP-associated pointed (minus) end of the actin polymer $k_{off}^- \sim 0.2 \text{ s}^{-1}$ (Fig. 2). Given that each G-actin monomer is $\sim 5 \text{ nm}$ in size, the actin polymer tip motion per unit time is then 1 nm/s , and the time taken to move $1 \mu\text{m}$ is about 10^3 s , which is $\sim 15 \text{ min}$. This is comparable with actin treadmill rates in other cell cytoskeletal contexts, lying between about a minute in filopodia (39,40) to an hour in stereocilia (41). Importantly, this is also consistent with the observed timescale of tens of minutes for myosin filaments to establish stacks across stress fibers (11), a process known to require actin polymerization and depolymerization.

RESULTS AND DISCUSSION

Estimate of contractility-induced registry force

A rough estimate of the dipole moment of each actomyosin unit (“sarcomere”) in a stress fiber with ~ 10 nonmuscle myosin filaments per unit, each with ~ 10 myosin heads, with each head exerting $\sim 1 \text{ pN}$ at a duty ratio of 10%, is (8) $P \sim 10 \text{ pN} \cdot \mu\text{m}$. This, together with $E = 10^4 \text{ Pa}$ as an estimate for cytoskeletal rigidity (42) and $d = 0.3 \mu\text{m}$ for stress fiber separation, gives an estimate of the registry force: $f_r \sim P^2/(\pi E d^4) \sim 0.3 \text{ pN}$. The factor by which rate constants are modified is then $\exp(f_r b/kT) \approx 1.5$, where $b \approx 5 \text{ nm}$ is about the monomer size. We use this estimate to show below that a combination of contractility-driven elastic interactions and actin (de)polymerization can explain the observed timescales at which an actomyosin unit moves into registry with another in a neighboring stress fiber.

Kinetic processes involved in myosin registry

Myosin filaments that initially were not registered with those on neighboring fibers tended to move into mutual registry on the scale of tens of minutes (11). Some typical processes involved in the formation of these myosin stacks are shown in the microscopy images in Figs. 4 and 5. In Fig. 4, a distant and distinct actin fiber associated with a few myosin filaments is drawn into and incorporated into an existing actin bundle with the resultant stacking of myosin. In

Fig. 5, two parallel stacks of myosin filaments move (in the direction parallel to their respective actin bundles) into mutual registry to form a wider stack that registers even more distinct and distant stress fibers. Both these processes involve long-range motion of actin and myosin and are thus likely to be driven by mechanical forces transmitted by the cytoskeleton. The previously described theoretical model of interacting actomyosin force dipoles explains the motion of myosin filaments toward registry as well as quite possibly the attractive force that draws the actin fiber in Fig. 4 into the pre-existing bundle. In Fig. 4, we track the position of the moving myosin filament in relation to a reference myosin in the pre-existing stack (yellow arrow), reminiscent of the model situation of a single dipole interacting with a line of dipoles in Fig. 1 D. Although the single actomyosin fiber moves with a speed of $\sim 0.1 \mu\text{m/min}$ (Fig. 4), the mutual registry of the two stacks in Fig. 5 is slower. This is intuitive because the motions of correlated myosin stacks involve a greater remodeling of the surrounding cytoskeleton, including the cross-linkers that connect the different actin filaments within a bundle. Furthermore, both these images indicate changes in the length of actin filaments associated with myosin. This illustrates that continuous polymerization and depolymerization of actin is indeed important for registry.

The timescales found from the microscopy experiments also rule out more naïve models for myosin registry kinetics in favor of our force-dependent polymerization model. For example, if the myosin filament were modeled as a cylindrical rod of length $L = 300 \text{ nm}$ and radius $r = 7.5 \text{ nm}$, being driven by a typical molecular-scale force of $f \sim \text{pN}$ through the cytoskeleton of viscosity, $\eta = 10 \text{ Pa} \cdot \text{s}$ (43), the resulting expected drift speed from usual Stokes-Einstein kinetics with a drag coefficient of $\Gamma = 6\pi\eta L/\log(2L/r) \sim \text{pN} \cdot \text{s/m}$ would be $f/\Gamma \sim 1 \mu\text{m/s}$, much higher than what is observed. Also, the sliding speed of the myosin motor filament of an actin filament is known to be 200 nm/s , which amounts to a motion of $10 \mu\text{m}$ per minute (1). Clearly, the motions of myosin tracked in the experimental images here are slower. We attribute this to the necessity for actin to polymerize and depolymerize during the myosin stacking process, as well as the binding and unbinding of the cross-linkers, which results in overall longer timescales.

We now explore in detail the polymerization/depolymerization kinetics of a single actin filament, e.g., the left filament shown in stress fiber B in Fig. 3. The rate of change of length of this filament depends on the filament tension as (30)

$$v = v_p \exp(fb/kT) - v_d, \quad (3)$$

where $v_p = k_{on} b c_a$ is the polymerization velocity at the barbed end of a tension-free actin filament that depends on the polymerization rate, effective monomer size, and concentration of free G-actin monomers, c_a ; f is the force

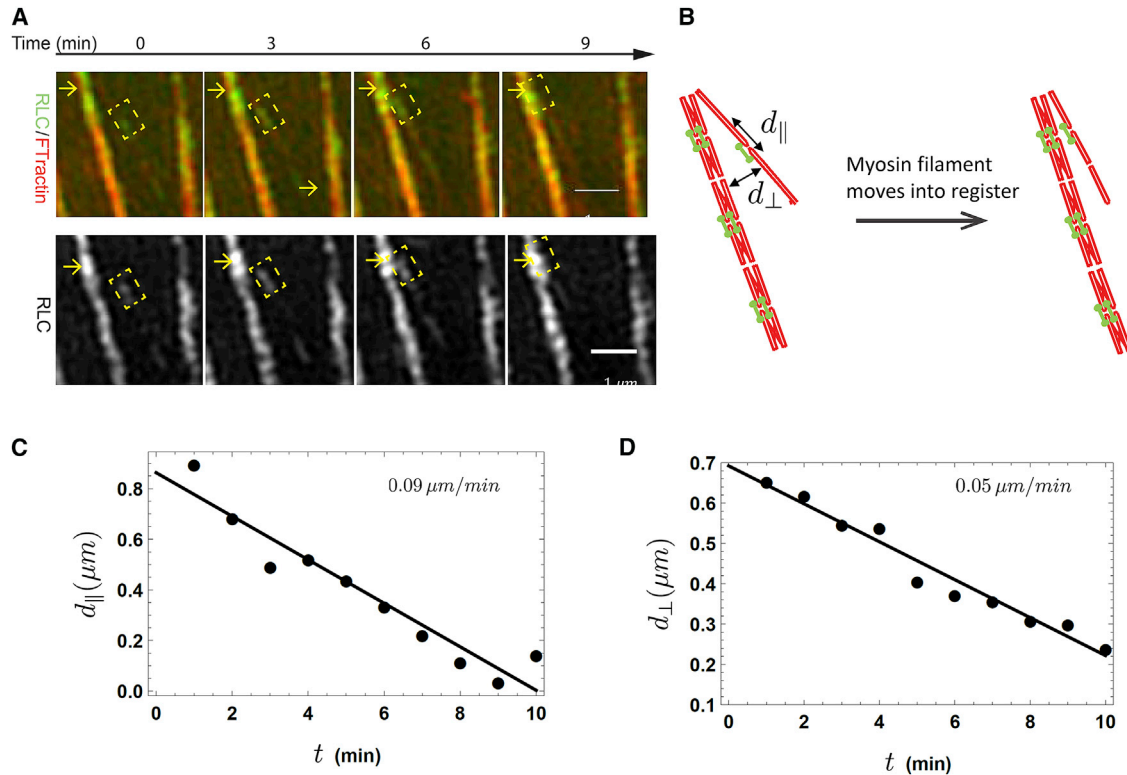


FIGURE 4 Experimental image of incorporation of myosin filament into stack. (A) A thin actin fiber (label: F-Tractin-tdTomato, red) with associated myosin filaments (myosin marked by its regulatory light chain, RLC-GFP, green) is drawn into an actin bundle with a pre-existing myosin stack (yellow arrow). Simultaneously, the myosin filament in the thin actin fiber (dashed rectangle) moves into register with the reference myosin (yellow arrow) on the thicker, pre-existing actin bundle on the left. The images, previously unpublished, were obtained with N-SIM microscopy in experiments reported in (11). (B) A cartoon showing the formation of myosin filament stacks via alignment with the pre-existing stack is given. Myosin filaments are in green, and associated actin bundles are in red. (C and D) Quantification of the myosin motions extracted from the microscopy, focusing on the myosin on the upper right and its displacements in reference to the fixed myosin, is shown. d_{\parallel} and d_{\perp} are distances traveled by the myosin along and transverse to the reference actin fiber. Both these displacements show a speed of nearly one micron in 10 min.

acting on the actin filament; and $v_d = k_{off}b$ is the depolymerization velocity at the pointed end. The forces act at the barbed ends and the force dependence of the kinetics is expected to be more pronounced for the more active barbed end. The effect of force on the depolymerization rate at the barbed end is assumed to be small and is thus ignored in Eq. 3, though this is easy to generalize without changing the model predictions qualitatively (29).

In the absence of registry force that biases the polymerization-depolymerization, there is no net motion or length changes of the actin filament. This implies that $v_p \exp(f_0 b/kT) = v_d$, where f_0 is the steady-state tensile force acting on each actin filament (from actomyosin contractility and other possible sources that keep the actin filament under tension). There is a registry force, f_r , from a neighboring actomyosin bundle that acts in addition to this steady-state force and breaks the symmetry between the actin polymers on either side of the myosin (Fig. 3). The registry force puts the actin on the left under tension and compresses the actin on the right. This increases the polymerization velocity on the left and lowers the polymerization velocity on the right:

$$v_{L,R} = v_p \exp((f_0 \pm f_r)b/kT) - v_d = v_d (\exp(\pm f_r b/kT) - 1), \tag{4}$$

where we make use of the steady-state balance of rates, $v_p \exp(f_0 b/kT) = v_d$, to cast the rate of change of length of the left and right actin filaments in terms of the registry force. The difference in sign of v_L and v_R indicates that the actin polymer on the left elongates and the one on the right shrinks, as depicted in the second panel of Fig. 3. The timescale for registry kinetics from mechanical force-modulated polymerization rates can then be estimated as $\tau_p \sim \Delta/|v_{L,R}|$. We previously estimated the registry force, $\exp(f_r b/kT) \approx 1.5$, which for $\Delta = 1 \mu\text{m}$ and $v_d = 5 \text{ nm/s}$ gives $\tau_p \sim 500 \text{ s} \sim 10 \text{ min}$, consistent with our previous simplified “rate-determining” timescale estimate.

Combined kinetics of adhesion, actin polymer, and the whole stress fiber

So far, we have focused on a particular actomyosin unit and considered how it moves under the action of registry forces

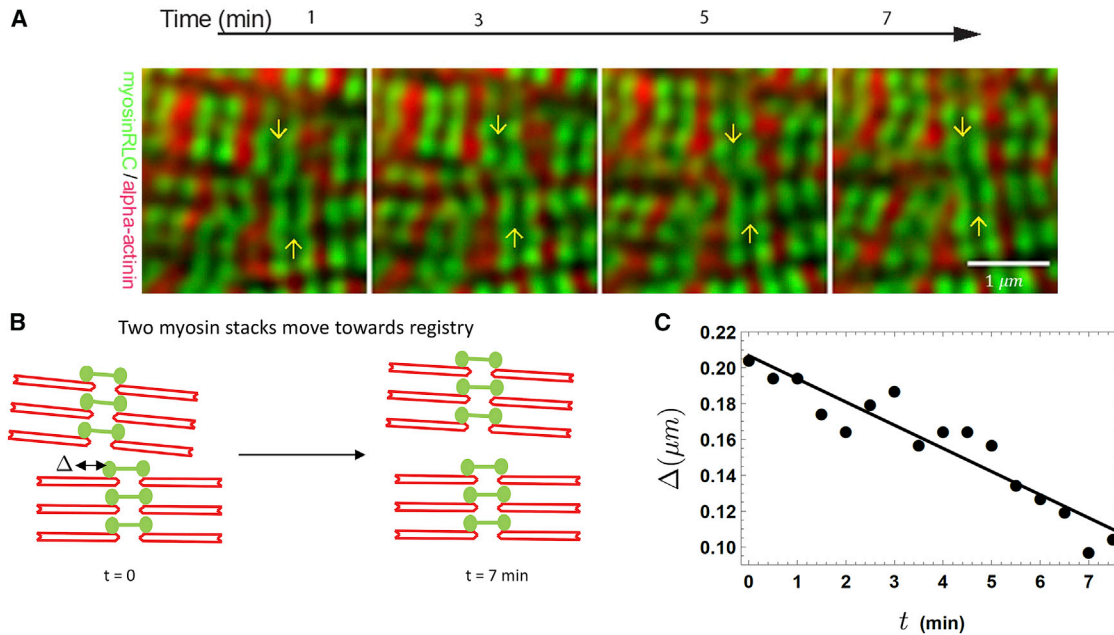


FIGURE 5 Experimental image of two merging myosin filament stacks. (A) Two nearly parallel stacks of myosin filaments (tracked by yellow arrows) on separate actin bundles move toward mutual registry along actin bundles to form a wider stack. Myosin is marked by its regulatory light chain, RLC-GFP (green), and α -actinin-1-mCherry (red) marks α -actinin, which is known to occur complementary to myosin along the actin bundle (11). Together, the red and green regions define the direction of the stress fibers in this image. The images, previously unpublished, were obtained with N-SIM microscopy in experiments reported in (11). (B) A cartoon showing the registry of two myosin stacks into a wider stack is given. Myosin filaments are in green, and actin polymers are in red. (C) Quantification of the motion of a myosin stack (upper yellow arrow) in relation to another myosin stack (bottom yellow arrow) is shown. Δ represents their mutual separation along the stress fibers, which is seen to change by $\sim 0.1 \mu\text{m}$ over 7 min in this event.

communicated from actomyosin units on a neighboring stress fiber by the IVN. However, it is apparent that for this actomyosin unit to move, the rest of the stress fiber to which it is connected (dashed lines in Fig. 3), needs to remodel. The rest of the stress fiber is anchored to a stiff substrate at both ends through stable focal adhesions (see Fig. 1). It can be deformed at short timescales but can also remodel at long timescales through the turnover of actin and actin-binding proteins, including cross-linkers in the adhesion regions. Such remodeling of elastic stress fibers has been shown by stimulating their contractility in optogenetic experiments (44). It is thus a viscoelastic entity that we describe with a one-dimensional Maxwell model comprising a spring of elastic modulus, E_s , connected in series to a dashpot with viscosity, η_s , as shown in the inset to Fig. 3. Such a model describes materials that both deform and flow under the application of mechanical forces. The effective motion of the actomyosin unit B that we have described can then be compensated for by a length change of the rest of the stress fiber that happens over longer timescales than involved in the remodeling of a single actomyosin unit. We now describe the combined kinetics of both the actomyosin unit B and the rest of the stress fiber connected to it through the adhesion zones.

As shown in Fig. 3, the net-force-induced displacement of an actomyosin unit B relative to a fixed unstressed fiber A is the sum of the length change of the associated actin poly-

mer, Δ_p , and the displacement of the α -actinin-rich adhesion region, which equals the stretch in the rest of the stress fiber, Δ_s . Both these processes reduce the registry mismatch distance, Δ (depicted as the stretch in the springs connecting stress fibers A and B in Fig. 3), and therefore, $d\Delta/dt = -d\Delta_s/dt - d\Delta_p/dt$.

The registry force acting on stress fiber B gives rise to a stress, and its change in length, Δ_s , gives rise to a strain. The force-displacement relationship suggested by a Maxwell model is therefore

$$\frac{df_r}{dt} + \frac{E_s}{\eta_s} f_r = k_s \frac{d\Delta_s}{dt}, \quad (5)$$

where an effective spring constant corresponding to the rest of the stress fiber may be defined as $E_s l_s \equiv k_s$, with l_s the unstressed length of the fiber, and η_s/E_s is a timescale associated with the remodeling of the rest of the stress fiber.

We wish to re-express Eq. 5 entirely in terms of the registry force, f_r , to give the dynamics of stress relaxation. We do so by writing the right-hand side of Eq. 5 as $d\Delta_s/dt = -d\Delta/dt - d\Delta_p/dt$. The instantaneous registry force depends on the distance by which an actomyosin unit is out of registry with respect to its neighbor, $f_r(\Delta(t))$, at that time. Using the force-based polymerization velocity for the left polymer that is lengthening under registry force, $v_L = d\Delta_p/dt$, derived in Eq. 4, we re-express the right-hand side of Eq. 5 as

$$\frac{df_r}{dt} + \frac{E_s f_r}{\eta_s} = -k_s \left(\frac{d\Delta(f_r)}{dt} + v_d (\exp(f_r b/kT) - 1) \right), \quad (6)$$

where the registry mismatch, Δ , can in principle be expressed in terms of the registry force, f_r , through an inversion of the expression in Eq. 2.

For the general dependence of f_r on the distance by which neighboring actomyosin units are out of registry, Δ (plotted for a single pair of dipoles in Fig. 1 C), the dynamics in Eq. 6 does not have a closed form expression in terms of f_r . In the limit that the misregistry is small or close to maximal ($\Delta \ll a$ or $|\Delta - a/2| \ll a$), the registry force in Eq. 2 can be linearized as $f_r = k_r \Delta$ (or $f_r = k_r(\Delta - a/2)$ in the case of nearly complete “antiregistry”). Thus, $d\Delta/dt = k_r^{-1} df_r/dt$. The “spring constant” depends on the elastic properties of the medium and the transverse separation of the actomyosin units: $k_r \sim P^2 |\phi| / (Ea^5)$. Further, because work done by registry force in moving actin by a single monomer length scale can be significantly smaller than the thermal energy (confirmed by our previous estimate of registry force less than 1 pN), $f_r b \ll kT$, its effect on the actin polymerization kinetics is linear in the registry force: $d\Delta_p/dt \approx v_d f_r b / (kT)$. Using both these linearized expressions in Eq. 6 and rearranging terms, we get an expression for the relaxation of stress in the stress fiber,

$$\frac{df_r}{dt} \left(1 + \frac{k_s}{k_r} \right) = -E_s (\eta_s^{-1} + \eta_p^{-1}) f_r, \quad (7)$$

where $\eta_p \equiv kT / (l_s v_d b)$ is an effective viscosity of the single actin polymer, which dissipates energy by adding or losing monomers in energy-consuming steps. The linearized stress fiber dynamics in Eq. 7 predicts an exponential relaxation of stress in the fiber as it moves toward the registered state, $f_r \sim \exp(-t/\tau)$, with a decay time of τ given by $\tau^{-1} = (1 + k_s/k_r)^{-1} \times E_s \times (\eta_s^{-1} + \eta_p^{-1})$. This gives the overall dynamics of registry, which depends on two processes, both induced by the registry force: the lengthening or shortening of the individual actin polymers within a “sarcomere” and the viscoelastic flow of the rest of the stress fiber. When these two relevant timescales (given by η_p and η_s) are well-separated, the dynamics is seen to be dictated by the shorter timescale. This is a consequence of the picture in Fig. 3 in which registry of actomyosin units may be completed by changes in length of the actin polymers within the actomyosin unit or that of the rest of the stress fiber. We expect the stress-fiber-remodeling timescales to be longer (tens of minutes to hours) than that of individual actin polymer turnover, based on stress fiber perturbation (44) and cell stretch (45) experiments. This agrees with the polymerization timescale of 10 min we estimated earlier and is also in line with the longer times required for correlated motions

of entire myosin stacks seen in Fig. 5 when compared to individual actomyosin motions seen in Fig. 4

CONCLUSIONS

Based on the experimental observation that actomyosin contractile activity and actin polymerization kinetics are both important for establishing registry of myosin filaments, we suggest that tension-modulated actin polymerization is responsible for registry kinetics. This allows actin filaments to lengthen and shorten in appropriate directions so as to translocate myosin filaments toward mutual registry. Because the translocation of myosin filaments under a registering force is highly stochastic and the rate-determining step for actin turnover is only about nm/s, the model predicts slow kinetics for the establishment of registry. This is consistent with the experimentally observed timescales of tens of minutes required for formation of myosin stacks in nonmuscle cells.

A detailed comparison of the model with existing experiments is precluded by the qualitative nature of knockdown and drug perturbation studies and our lack of knowledge of the material properties and exact composition of the IVN. Although disordered, loosely organized actin has been imaged between stress fibers, we cannot in principle rule out the contribution of other cytoskeletal components such as intermediate filaments or microtubules to the IVN. The knockdown of actin-associated proteins affects both the actin part of the IVN, including its rigidity, E , as well as the stress fibers and their material properties: the stress fiber elastic modulus, E_s , and viscosity, η_s . The knockdown of intermediate filaments may, on the other hand, be a strategy to independently perturb the IVN.

Although we cannot model the results of knockdown experiments in quantitative detail, we now qualitatively discuss the key role of two actin-binding proteins in myosin stacking as discovered in (11). Knockdown of a particular formin, Fmnl3, disrupts myosin stacks, consistent with the well-known role of formins in actin filament growth and the observation that actin polymerization is crucial for myosin stack formation. Although certain formins such as mDia1 have been demonstrated in vitro to facilitate force-dependent growth of actin (33,34), similar studies specifically on Fmnl3 or on a comprehensive knockdown of different formins present in stress fibers in the cell are lacking. In the absence of direct evidence that formin-mediated effects of force on actin elongation are important in the cell, our model relies on a general thermodynamic argument for the force dependence of actin polymerization rates that is independent of the detailed molecular mechanism (28,29). However, we do point out that these arguments may be extended to describe the effect of forces on formin, particularly on the elastic ring-like FH2 domain of formins whose conformation is thought to be force-modulated (34,46,47). In our model, this can be accounted for by a force-dependent

k_{on} in Eq. 3, which will be enhanced by a factor of $\exp(f_r \Delta_f / kT)$, where Δ_f is the displacement associated with the conformational change of the elastic FH2 domain of formin. The effect of knockdown of the actin cross-linker α -actinin is qualitatively consistent with our model, though it is not a direct evidence of the importance of mechanical force transmission. α -actinin-4 knockdown is seen to have a dramatic effect on the organization of the actin bundles, resulting in the formation of fewer but thicker stress fibers because the actin filaments pack closer together in the absence of the large α -actinin cross-linker (11). Neighboring stress fibers that are further apart and a sparser IVN imply reduced transmission of mechanical forces between them. This is readily seen from Eq. 2, in which increased transverse separation between fibers, d , leads to a smaller force transmission factor, $\phi(d/a)$ and consequently lower registry forces f_r acting on individual actomyosin units. Perturbation of α -actinin could also affect other factors in the model, such as the polymerization rates of actin.

The theoretical picture presented here relates observations from a cell biology experiment to parameters measurable in single molecule experiments of actin polymerization kinetics and actomyosin physicochemical activity. The model quantitatively predicts how the registry timescale should vary with the mechanical properties of the medium and the polymerization rate of actin. These may be verified in principle by experimental probes that can tune these parameters in a controlled manner. Knowing other parameters, the model provides a way to estimate adhesion remodeling times. For example, the experimental observation that striation is established in developing embryonic muscle tissue over the course of days (48) instead of hours may indicate that adhesion remodeling times are much longer in muscle tissue. Over such timescales, biological or genetic changes may also occur in cells in addition to the purely physical changes in cytoskeletal architecture that we consider here. Tension in the actin filaments may also affect myosin binding rates (49) and reinforce the contractile activity that is responsible for registry forces. Our model can be extended to incorporate such molecular mechanosensitive feedback effects once future research is done to quantify those effects in isolated actin filaments.

SUPPORTING MATERIAL

Supporting Material can be found online at <https://doi.org/10.1016/j.bpj.2019.07.040>.

AUTHOR CONTRIBUTIONS

All authors performed research and wrote this article.

ACKNOWLEDGMENTS

We thank Ajay Gopinathan, Jing Xu, Nir Gov, and Patrick Oakes for useful comments and discussion.

K.D. acknowledges support from the NSF-CREST: Center for Cellular and Biomolecular Machines at UC Merced (NSF-HRD-1547848).

A.D.B. acknowledges support from the National Research Foundation, Prime Minister's Office, Singapore, and the Ministry of Education under the Research Centres of Excellence program through the Mechanobiology Institute, Singapore (Ref no. R-714-006-006-271) and Singapore Ministry of Education Academic Research Fund Tier 3 MOE Grant No. MOE2016-T3-1-002, as well as from Maimonides Israeli-France grant (Israeli Ministry of Science Technology and Space) and EU Marie Skłodowska-Curie Network InCeM (Project ID: 642866) at the Weizmann Institute of Science.

S.A.S acknowledges the support of the Israel Science Foundation, the US-Israel Binational Science Foundation, the Henry Kreuter Institute for Biomedical Imaging and Genomics, and support of the Kretzner-Katz and Perlman Family Foundations. Prof. Safran is the incumbent of the Fern & Manfred Steinfeld Professorial Chair.

REFERENCES

- Howard, J. 2001. *Mechanics of Motor Proteins and the Cytoskeleton*. Sinauer Associates, Sunderland, MA.
- Zemel, A., F. Rehfeldt, ..., S. A. Safran. 2010. Optimal matrix rigidity for stress fiber polarization in stem cells. *Nat. Phys.* 6:468–473.
- Balaban, N. Q., U. S. Schwarz, ..., B. Geiger. 2001. Force and focal adhesion assembly: a close relationship studied using elastic micropatterned substrates. *Nat. Cell Biol.* 3:466–472.
- Discher, D. E., P. Janmey, and Y. L. Wang. 2005. Tissue cells feel and respond to the stiffness of their substrate. *Science*. 310:1139–1143.
- Schwarz, U. S., and S. A. Safran. 2002. Elastic interactions of cells. *Phys. Rev. Lett.* 88:048102.
- Schwarz, U. S., and S. A. Safran. 2013. Physics of adherent cells. *Rev. Mod. Phys.* 85:1327–1381.
- Lemke, S. B., and F. Schnorrer. 2017. Mechanical forces during muscle development. *Mech. Dev.* 144:92–101.
- Friedrich, B. M., A. Buxboim, ..., S. A. Safran. 2011. Striated actomyosin fibers can reorganize and register in response to elastic interactions with the matrix. *Biophys. J.* 100:2706–2715.
- Dasbiswas, K., S. Majkut, ..., S. A. Safran. 2015. Substrate stiffness-modulated registry phase correlations in cardiomyocytes map structural order to coherent beating. *Nat. Commun.* 6:6085.
- Hotulainen, P., and P. Lappalainen. 2006. Stress fibers are generated by two distinct actin assembly mechanisms in motile cells. *J. Cell Biol.* 173:383–394.
- Hu, S., K. Dasbiswas, ..., A. D. Bershadsky. 2017. Long-range self-organization of cytoskeletal myosin II filament stacks. *Nat. Cell Biol.* 19:133–141.
- Fenix, A. M., N. Taneja, ..., D. T. Burnette. 2016. Expansion and concatenation of non-muscle myosin IIA filaments drive cellular contractile system formation during interphase and mitosis. *Mol. Biol. Cell.* 27:1465–1478.
- Beach, J. R., K. S. Bruun, ..., J. A. Hammer. 2017. Actin dynamics and competition for myosin monomer govern the sequential amplification of myosin filaments. *Nat. Cell Biol.* 19:85–93.
- Hu, S., H. Grobe, ..., R. Zaidel-Bar. 2019. Reciprocal regulation of actomyosin organization and contractility in nonmuscle cells by tropomyosins and alpha-actinins. *Mol. Biol. Cell.* 30:2025–2036.
- Jiu, Y., R. Kumari, ..., P. Lappalainen. 2019. Myosin-18B promotes the assembly of myosin II stacks for maturation of contractile actomyosin bundles. *Curr. Biol.* 29:81–92.e5.
- Engler, A. J., M. A. Griffin, ..., D. E. Discher. 2004. Myotubes differentiate optimally on substrates with tissue-like stiffness: pathological implications for soft or stiff microenvironments. *J. Cell Biol.* 166:877–887.

17. Weitkunat, M., A. Kaya-Çopur, ..., F. Schnorrer. 2014. Tension and force-resistant attachment are essential for myofibrillogenesis in *Drosophila* flight muscle. *Curr. Biol.* 24:705–716.
18. Dasbiswas, K., S. Hu, ..., A. D. Bershadsky. 2018. Ordering of myosin II filaments driven by mechanical forces: experiments and theory. *Philos. Trans. R. Soc. Lond. B Biol. Sci.* 373:20170114.
19. Harris, A. R., P. Jreij, and D. A. Fletcher. 2018. Mechanotransduction by the actin cytoskeleton: converting mechanical stimuli into biochemical signals. *Annu. Rev. Biophys.* 47:617–631.
20. Rhee, D., J. M. Sanger, and J. W. Sanger. 1994. The premyofibril: evidence for its role in myofibrillogenesis. *Cell Motil. Cytoskeleton.* 28:1–24.
21. McClure, D. B., M. J. Hightower, and W. C. Topp. 1982. Effect of SV40 transformation on the growth requirements of the rat embryo cell line REF52 in serum-free medium. *Cold Spring Harbor Conf., Cell Proliferation.* 9:345–364.
22. Xu, K., H. P. Babcock, and X. Zhuang. 2012. Dual-objective STORM reveals three-dimensional filament organization in the actin cytoskeleton. *Nat. Methods.* 9:185–188.
23. Landau, L. D., and E. M. Lifshitz. 1959. *Theory of Elasticity, Volume 7 of Course of Theoretical Physics.* Pergamon Press, London, UK.
24. Yuval, J., and S. A. Safran. 2013. Dynamics of elastic interactions in soft and biological matter. *Phys. Rev. E Stat. Nonlin. Soft Matter Phys.* 87:042703.
25. Phillips, R., J. Kondev, and J. Theriot. 2008. *Physical Biology of the Cell.* Garland Science, Taylor & Francis Group, New York.
26. Pollard, T. D. 1986. Rate constants for the reactions of ATP- and ADP-actin with the ends of actin filaments. *J. Cell Biol.* 103:2747–2754.
27. Mogilner, A., and G. Oster. 1996. Cell motility driven by actin polymerization. *Biophys. J.* 71:3030–3045.
28. Hill, T. L., and M. W. Kirschner. 1982. Bioenergetics and kinetics of microtubule and actin filament assembly-disassembly. *Int. Rev. Cytol.* 78:1–125.
29. Gerbal, F., P. Chaikin, ..., J. Prost. 2000. An elastic analysis of *Listeria* monocytogenes propulsion. *Biophys. J.* 79:2259–2275.
30. Mogilner, A., and G. Oster. 2003. Force generation by actin polymerization II: the elastic ratchet and tethered filaments. *Biophys. J.* 84:1591–1605.
31. Bell, G. I. 1978. Models for the specific adhesion of cells to cells. *Science.* 200:618–627.
32. Courtemanche, N., J. Y. Lee, ..., E. C. Greene. 2013. Tension modulates actin filament polymerization mediated by formin and profilin. *Proc. Natl. Acad. Sci. USA.* 110:9752–9757.
33. Jégou, A., M. F. Carlier, and G. Romet-Lemonne. 2013. Formin mDia1 senses and generates mechanical forces on actin filaments. *Nat. Commun.* 4:1883.
34. Yu, M., X. Yuan, ..., J. Yan. 2017. mDia1 senses both force and torque during F-actin filament polymerization. *Nat. Commun.* 8:1650.
35. Bieling, P., T. D. Li, ..., R. D. Mullins. 2016. Force feedback controls motor activity and mechanical properties of self-assembling branched actin networks. *Cell.* 164:115–127.
36. Pollard, T. D., and G. G. Borisy. 2003. Cellular motility driven by assembly and disassembly of actin filaments. *Cell.* 112:453–465.
37. Shemesh, T., B. Geiger, ..., M. M. Kozlov. 2005. Focal adhesions as mechanosensors: a physical mechanism. *Proc. Natl. Acad. Sci. USA.* 102:12383–12388.
38. Murrell, M., P. W. Oakes, ..., M. L. Gardel. 2015. Forcing cells into shape: the mechanics of actomyosin contractility. *Nat. Rev. Mol. Cell Biol.* 16:486–498.
39. Zidovska, A., and E. Sackmann. 2011. On the mechanical stabilization of filopodia. *Biophys. J.* 100:1428–1437.
40. Orly, G., M. Naoz, and N. S. Gov. 2014. Physical model for the geometry of actin-based cellular protrusions. *Biophys. J.* 107:576–587.
41. Naoz, M., U. Manor, ..., N. S. Gov. 2008. Protein localization by actin treadmilling and molecular motors regulates stereocilia shape and treadmilling rate. *Biophys. J.* 95:5706–5718.
42. Takai, E., K. D. Costa, ..., X. E. Guo. 2005. Osteoblast elastic modulus measured by atomic force microscopy is substrate dependent. *Ann. Biomed. Eng.* 33:963–971.
43. Kollmannsberger, P., and B. Fabry. 2011. Linear and nonlinear rheology of living cells. *Annu. Rev. Mater. Res.* 41:75–97.
44. Oakes, P. W., E. Wagner, ..., M. L. Gardel. 2017. Optogenetic control of RhoA reveals zyxin-mediated elasticity of stress fibres. *Nat. Commun.* 8:15817.
45. Livne, A., E. Bouchbinder, and B. Geiger. 2014. Cell reorientation under cyclic stretching. *Nat. Commun.* 5:3938.
46. Kozlov, M. M., and A. D. Bershadsky. 2004. Processive capping by formin suggests a force-driven mechanism of actin polymerization. *J. Cell Biol.* 167:1011–1017.
47. Shemesh, T., and M. M. Kozlov. 2007. Actin polymerization upon processive capping by formin: a model for slowing and acceleration. *Biophys. J.* 92:1512–1521.
48. Engler, A. J., C. Carag-Krieger, ..., D. E. Discher. 2008. Embryonic cardiomyocytes beat best on a matrix with heart-like elasticity: scar-like rigidity inhibits beating. *J. Cell Sci.* 121:3794–3802.
49. Greenberg, M. J., G. Arpağ, ..., E. M. Ostap. 2016. A perspective on the role of myosins as mechanosensors. *Biophys. J.* 110:2568–2576.